Published in "Pathogens and Disease doi: 10.1111/2049-632X.12065, 2013"
which should be cited to refer to this work.

Early expression of the type III secretion system of *Parachlamydia acanthamoebae* during a replicative cycle within its natural host cell *Acanthamoeba castellanii*

Antony Croxatto, Valérie Murset, Bérénice Chassot & Gilbert Greub

Center for Research on Intracellular Bacteria (CRIB), Institute of Microbiology, University Hospital Center and University of Lausanne, Lausanne, Switzerland

In this innovative study, the type three secretion system genes in the ancient organism, *Parachlamydia acanthamoebae* were studied in its natural host, amoeba. Interestingly, the putative T3SS genes in *Parachlamydia* are similar to those in modern chlamydiae and were found to be maximally expressed in the early and mid stages of the infection cycle, indicating their critical role in subverting pathways in their host.

Keywords
intracellular bacteria; type III secretion system; *Chlamydia*.

Correspondence
Gilbert Greub, Center for Research on Intracellular Bacteria, Institute of Microbiology, University Hospital Center and University of Lausanne, 1011 Lausanne, Switzerland.
Tel.: (00) 41 21 314 49 79
fax: (00) 41 21 314 40 60
e-mail: gilbert.greub@chuv.ch

Present address: Valérie Murset, Institute of Microbiology, ETH Zürich, Zürich, Switzerland

Present address: Bérénice Chassot, Zoology, Department of Biology, University of Fribourg, Fribourg, Switzerland

Abstract

The type three secretion system (T3SS) operons of *Chlamydiales* bacteria are distributed in different clusters along their chromosomes and are conserved at both the level of sequence and genetic organization. A complete characterization of the temporal expression of multiple T3SS components at the transcriptional and protein levels has been performed in *Parachlamydia acanthamoebae*, replicating in its natural host cell *Acanthamoeba castellanii*. The T3SS components were classified in four different temporal clusters depending on their pattern of expression during the early, mid- and late phases of the infectious cycle. The putative T3SS transcription units predicted in *Parachlamydia* are similar to those described in *Chlamydia trachomatis*, suggesting that T3SS units of transcriptional expression are highly conserved among *Chlamydiales* bacteria. The maximal expression and activation of the T3SS of *Parachlamydia* occurred during the early to mid-phase of the infectious cycle corresponding to a critical phase during which the intracellular bacterium has (1) to evade and/or block the lytic pathway of the amoeba, (2) to differentiate from elementary bodies (EBs) to reticulate bodies (RBs), and (3) to modulate the maturation of its vacuole to create a replicative niche able to sustain efficient bacterial growth.

Introduction

The *Chlamydiales* order currently includes the *Chlamydiaceae*, *Parachlamydiaceae, Waddliaceae*, *Simkaniaceae*, *Criblamydiaceae*, and *Rhabdochlamydiaceae* families (Corsaro & Greub, 2006).

Parachlamydiaceae naturally resist destruction by free-living amoebae. These obligate intracellular bacteria may use the protistan host as a training ground to select virulence traits that help them to resist the microbicidal effectors of amoebae and macrophages (Greub & Raoult, 2004; Greub, 2009). *Parachlamydia acanthamoebae* is a bacterium belonging to the *Parachlamydiaceae* family. *P. acanthamoebae* is seriously suspected to be involved in respiratory tract infections (Greub, 2009; Lamoth & Greub, 2009) since serological and molecular evidences are supporting its role as a human respiratory pathogen, mainly in patients with community-acquired (Greub *et al*., 2003b) and aspiration pneumonia (Greub *et al.*, 2003c). In addition, the disease has been reproduced in a murine model following both intranasal and intratracheal bacterial inoculation (Casson *et al*., 2008).

The pathogenic potential of *Parachlamydia* is further supported by the ability of these obligate intracellular bacteria to enter and replicate in human macrophages (Greub *et al.*, 2003a), by preventing the secretion of proinflammatory cytokines (Greub *et al.*, 2005a) and the fusion of its endocytic vacuole with the lysosome (Greub *et al.*, 2005b). Moreover, *Parachlamydia* is also able to enter and replicate in pneumocytes and lung fibroblasts (Casson *et al.*, 2006).

Members of the *Chlamydiales* are characterized by a biphasic development cycle comprising the infectious elementary bodies (EBs) and the replicating reticulate bodies (RBs). They have evolved from a common ancestor since more than 700 million years (Greub & Raoult, 2003) that has developed mechanisms for intracellular survival and multiplication in primitive unicellular eukaryotes. Consequently, *Chlamydia*-related bacteria and classical *Chlamydia* share a 'core genome' of about 700 ORFs that encode for essential bacterial functions that guarantee an efficient intracellular lifestyle including several virulence mechanisms such as the type III secretion system (T3SS) (Horn *et al.*, 2004; Greub *et al.*, 2009; Bertelli *et al.*, 2010; Collingro *et al.*, 2011b).

T3SS mediates the translocation of bacterial effectors to the cytosol of infected cells to modulate various host cell functions facilitating the survival and the replication of the bacterial pathogens (Coburn *et al.*, 2007). The proteins that constitute the T3SS secretory apparatus are termed 'structural proteins'. An additional set of proteins termed 'translocators' function by translocating virulence factors called 'effector' proteins into the host cell cytoplasm. T3SS genes are present in all *Chlamydia* species examined to date and suggest that T3SS is essential for the survival of these strict intracellular bacteria. Proteins that compose the T3SS secretory apparatus and translocators are for the most part well conserved structurally and functionally among *Chlamydiales* spp., and genes encoding for these T3SS proteins are found in distinct conserved genomic clusters (Peters *et al.*, 2007; Betts *et al.*, 2008a). In contrast, T3SS effectors display little sequence homology and are much harder to identify, except for some members of the family of T3SS-secreted Inc proteins that are characterized by a large bilobed hydrophobic domain that serves to anchor the proteins in the inclusion membrane (Bannantine *et al.*, 2000). Effectors being the direct modulators of host cell functions and of unique pathogenic properties, every bacterium has adapted its pool of effectors to survive and replicate in their respective environmental niches, which likely explained the poor sequence conservation among these secreted proteins. However, effector proteins often display common structural traits and have similar enzymatic activities among various bacterial species, including cytoskeletal rearrangement, subversion of signaling pathways, activation or inhibition of apoptosis, and modulation of intracellular trafficking (Mota & Cornelis, 2005). In *Chlamydiales*, effector proteins are secreted in the inclusion lumen, inserted in the inclusion membrane or translocated in the cytosol of the host cell. A few effectors have been identified so far in *Chlamydiaceae* including Tarp, inclusion membrane proteins IncA to IncG, CADD, Mip, and CopN (Bannantine *et al.*, 2000; Subtil *et al.*, 2005; Beeckman & Vanrompay, 2010).

The secretory apparatus is composed of about 20 proteins. The functions of the proteins that compose the injectisome of *Chlamydiales* bacteria have been mainly attributed based on sequence similarities with proteins composing well-described heterologous T3SS apparatus of other bacteria species such as *Yersinia* and *Salmonella* (Hueck, 1998). Several studies indicate that the secretin-like SctC protein forms the outer membrane (OM) ring that is connected with the inner membrane (IM) ring through SctD. The (IM) ring is formed by SctD together with the lipoprotein SctJ. In the *Yersinia* T3SS apparatus, the IM ring is associated with a multicomponent complex composed of (1) SctR/S/T/U/V (proteins associated with the export apparatus), (2) Sct N/L (ATPase-associated proteins); and (3) SctQ which form the cytosolic ring (C ring) (Cornelis, 2002; Diepold *et al.*, 2010). Several studies focusing on T3SS protein interactions in *Chlamydia* indicate that the *Chlamydiales* T3SS apparatus is very similar in structure and function compared with the well-studied apparatus of *Yersinia* and other species (Fields & Hackstadt, 2006; Betts-Hampikian & Fields, 2010).

Recent experimental evidences obtained in the *Yersinia* model suggest that the apparatus assembly is initiated by the formation of the SctC OM ring and proceed inwards through the assembly of the IM ring SctD and SctJ. Upon completion of the IM ring, additional T3SS components are recruited to the basal apparatus to complete the export apparatus and to form the ATPase and C ring complexes. Finally, the needle consisted of SctF is assembled to form a mature and functional T3SS. Unlike SctN/L/Q, the exact temporal integration of the IM proteins SctR/S/T/U/V remained unclear (Diepold *et al.*, 2010).

Considering the central role of T3SS in *Chlamydiales* biology, a thorough characterization of T3SS expression of conserved components throughout an infectious cycle of *Parachlamydia* within *Acanthamoeba castellanii* amoeba was conducted. We showed that T3SS conservation among *Chlamydiales* is not only restricted to genomic sequence and organization but also observed at the level of temporal expression during the development cycle.

Materials and methods

Bacterial strain

Parachlamydia acanthamoebae strain Hall's coccus was grown at 32 °C within *A. castellanii* in 75-cm^2 cell culture flasks (Corning, New York, NY) with 30 mL of peptone–yeast extract–glucose broth (Greub & Raoult, 2002). After 5 days of incubation, cultures were harvested, and the broth was filtered through a 5-μm pore to eliminate both amoebal trophozoites and cysts and to collect bacteria in the flow through. *A. castellanii* ATCC 30010 was cultured in 75-cm^2 cell culture flasks at 25 °C.

Infection procedure

Amoebae harvested from 24-h fresh culture were centrifuged at 200 ***g*** for 5 min, resuspended in RPMI-HEPES

supplemented with 200 mM L-glutamine (Gibco-BRL, Life Technologies, Paisley, Scotland) and 10% fetal calf serum (Gibco-BRL). Then, 10^5 ameba cells mL^{-1} were incubated for 2 h at 25 °C in 24-well cell culture plates (Corning). Nonadherent cells were washed, and the remaining adherent cells were incubated for 16 h at 25 °C.

The amount of bacteria after 5 days of amoebal co-culture was equal to about 10^8 cells per mL as measured by quantitative PCR of the 16S rRNA gene. Host cell lysis assay following infection of *A. castellanii* with limiting serial dilution of a bacterial filtrate confirmed that most collected bacteria are living cells.

Wells containing 10^5 amoebae were infected with a 10^6 bacteria mL^{-1} suspension corresponding to a multiplicity of infection (MOI) of about 10. Plates were centrifuged at 1790 ***g*** for 10 min at room temperature. After 30 min of incubation at 32 °C, amoebal cells were washed with RPMI-HEPES and further incubated for different periods at 32 °C in RPMI-HEPES supplemented with 200 mM L-glutamine and 10% fetal calf serum.

Confocal microscopy

Infected amoebae were washed with PBS, fixed with ice-cold methanol for 4 min. Cells were then washed three times with PBS and were then blocked and permeabilized for 1 h in a blocking solution (PBS/0.1% Saponin/10% fetal calf serum). Coverslips were incubated with primary mouse antisera directed against different specific proteins (CopB, SycD1, Mcsc, SctW, SctJ, PahN) or against total whole cells of *Parachlamydia* for 1 h at room temperature in blocking solution. After washing three times with PBS/0.1% saponin, coverslips were incubated for 1 h with secondary anti-mouse antibodies in blocking solution containing concanavalin A (Invitrogen, Basel, Switzerland) and DAPI (dilactate, D3571; Molecular Probes, OR) to counterstain amoebae and label DNA, respectively. After two washing in PBS/0.1% saponin, two in PBS, and one with deionized water, the coverslips were mounted onto glass slides using Mowiol (Sigma-Aldrich, MO). Cells were observed on a confocal fluorescence microscope (Zeiss LSM710 Meta, Jena, Germany). Files were analyzed using ImageJ for microscopy (www.macbiophotonics.ca) software. All the assays were performed at least in triplicate.

Quantitative reverse transcription–polymerase chain reaction (qRT-PCR)

Amoebae were infected in 24-well plates as described before. Samples were harvested at different times post-infection by scraping amoeba cells from the well surface and by resuspending the samples in RNAprotect bacteria reagent (Qiagen GmbH, Germany). Total RNA was extracted using the RNeasy plus mini kit (Qiagen GmbH) as described by the manufacturer. The RNA samples were treated with the DNA-free kit (Ambion; Applied Biosystems, CA) to remove contaminating DNA from the RNA preparation.

The analysis of mRNA quantification was performed by a one-step reverse transcription–polymerase chain reaction using the one-step MESA GREEN qRT-PCR MasterMix Plus for SYBR® assay (Eurogentec, Seraing, Belgium). The design of the specific primers listed in Supporting Information, Table S1 was done with the Primer3plus software (http://primer3.sourceforge.net/webif.php). The qRT-PCR assay was performed in a total volume of 20 μL with 10 μL of 2x reaction buffer, 100 nM forward primer, 100 nM reverse primer, 0.25U μL^{-1} Euroscript reverse transcriptase, 0.1U μL^{-1} RNase inhibitor, and RNase-free water. The thermocycling conditions were set up as follows: (1) reverse transcription, 30 min, 48 °C, (2) Meteor *Taq* activation and Euroscript inactivation, 5 min, 95 °C, (3) 40 cycles, 15 s, 95 °C, 1 min, 60 °C, (4) melt curve analysis, temperature increment of 0.3% from 60 to 95 °C. The analysis of the 16S rRNA gene was used as an internal control to normalize the quantification of every specific mRNA collected at different times during an infectious cycle. The results are presented as a relative quantification taking samples at time 0 (EBs) as a reference of 1. Water was used as a negative control, and the qRT-PCR reaction without reverse transcriptase was used as a control to measure DNA contamination in the extracted RNA samples. All measurements were performed at least in triplicates.

Protein purification and generation of antisera

Parachlamydia acanthamoebae sctJ, *sctW*, *copB*, *mcsc*, *pah-N*, and *sycD1 (scc2)* ORFs were amplified from purified *P. acanthamoebae* genomic DNA using primers listed in Table S2 using the high-fidelity Phusion polymerase (Finnzymes, Espoo, Finland). Using the Champion pET directional TOPO expression kits (Invitrogen), *sctJ* and *mcsc* were cloned in frame with a N-terminal and C-terminal peptide containing a polyhistidine (6xHis) tag to generate the plasmids pET200/D-TOPO-*sctJ* and pET101/D-TOPO-*mcsc*, respectively (Table S2). The four bases (CACC) were added to the forward primers to allow directional in-frame cloning of the PCR fragments into plasmids pET200/D-TOPO and pET101/D-TOPO. Following digestion of the PCR amplicons and the plasmids with NcoI/HindIII, *copB* (nt 1–960) and *pahN* were ligated into the plasmid pBADmycHis (Invitrogen) to generate the plasmids pBADmycHis-*copB* and pBADmycHis-*pahN* encoding for C-terminal polyhistidine tag (6xHis) recombinant proteins. Similarly, *copN* and *sycD1 (scc2)* amplicons and the plasmid pET28a were digested with NdeI/BamHI to generate by ligation the plasmids pET28a-*copN* and pET28a-*sycD1 (scc2)* encoding for N-terminal polyhistidine tag recombinant proteins. The proteins were expressed in BL21 star (DE3) *Escherichia coli* strains following 0.5 mM IPTG (pET200/D-TOPO-*sctJ*/pET101/D-TOPO-*mcsc*/pET28a-*copN*/pET28a-*sycD1*) induction at 37 °C or in TOP10 *E. coli* strains following 0.02% arabinose (pBADmycHis-*copB*/pBADmycHis-*pahN*) induction at 37 °C. The BL21 and TOP10 *E. coli* strains expressing the protein of interest were lysed with the FastBreak cell lysis solution (Promega), and recombinant His-tagged proteins were purified in native or denaturing conditions using the

MagneHis protein purification system (Promega) according to the manufacturer's recommendation. Purified recombinant His-tagged proteins were used to conduct mouse immunization programs at the Eurogentec animal facility (Eurogentec, Seraing, Belgium) to elicit the production of specific mouse antisera.

Western blot

For immunoblot analysis, protein samples were separated by SDS-PAGE, transferred to 0.45-μm nitrocellulose membranes and blocked with 5% nonfat powder milk in TBST (50 mM Tris-base, 150 mM NaCl, 0.2% Tween pH 7.4). The nitrocellulose membranes were incubated with mouse primary antibodies (anti-SctJ, anti-SctW, anti-CopB, anti-Mcsc, anti-SycD1 and anti-Parachlamydia) diluted in 0.5% milk–TBST, washed 3 times, incubated with secondary antibody conjugated to horseradish peroxidase diluted in 0.5% milk–TBST, and detected by chemiluminescence. The density of the bands on Western blots was measured with the gel analysis method of the ImageJ software as described by Luke Miller (http://lukemiller.org/index.php/2010/11/analyzing-gels-and-western-blots-with-image-j/). Western blot have been done at least in triplicates for each analyzed proteins.

Quantitative immunofluorescence

Proteins were labeled by immunofluorescence staining with specific mouse polyclonal antibodies as described in confocal microscopy. A series of images of multiple focal planes covering the entire thickness of the sample were collected by *z*-stack confocal microscopy. Using the ImageJ software, a *Z* projection composed of the summing of the slices was generated. The region of interest (ROI) including only the signal of intensity emitted by the bacteria was defined by applying a median filter (2×2.0 pixels) and by adjusting the isodata threshold set-up. A histogram of the ROI composed of the signal intensity on the *x*-axis and of the frequency on the *y*-axis was generated. A mean value and a standard deviation of the histogram of the frequency distribution of fluorescence intensity were also generated. The results were then exported and analyzed using GraphPad Prism, version 5.00 for Windows (GraphPad Software, San Diego, CA). The signal intensity for each frequency was normalized using a value of 100 for the highest intensity. Several images from one experiment performed at least in triplicates have been analyzed for each protein.

Results

Temporal characterization of an infectious cycle

A thorough characterization of the different stages that compose a complete infectious cycle of *Parachlamydia* within *A. castellanii* was required to accurately define temporal key stages of the internalization, differentiation, replication, and extrusion of *Parachlamydia* during a replicative cycle. Amoebae were infected with a MOI of 10 to ensure a nearly 100% rate of infection allowing thus the study of a single replication cycle. The time course of the infection was similar between a MOI of 10 and 1, demonstrating that the MOI is not significantly affecting the growth kinetic of *Parachlamydia* within its natural host *A. castellanii* (Fig. S1). As shown by confocal microscopy, between 5 and 10 infectious bacteria were internalized into amoebae 1 h postinfection (Fig. 1a). The differentiation of EBs into RBs was mostly completed 5 h postinfection, and inclusions containing multiple replicating bacteria were observed 8 h postinfection. Following a lag phase characterized by the differentiation of EBs into RBs, an exponential growth is observed between 5 and 16 h postinfection as shown by quantitative PCR (Fig. 1b). The bacterial growth enters stationary phase between 16 h and 24 h postinfection, which corresponds to the beginning of the redifferentiation of RBs into EBs (Fig. 1a and b). As shown in Fig. 1a, most of the amoebae are lysed 48 h postinfection, releasing EBs in the extracellular environment. Based on these data, the infectious cycle was classified as early, mid-, and late cycles. These times correspond to key developmental stages with (1) early cycle during which bacteria are internalized in the host cell and differentiate from EBs into RBs, (2) mid-cycle characterized by exponential growth of dividing RBs, and (3) late cycle consisting of the end of bacterial growth, redifferentiation of RBs into EBs, and finally release of EBs into the extracellular environment (Fig. 1c).

Identification of 16S rRNA gene as an optimal internal control to measure relative transcriptional expression during a replicative cycle

Chlamydiales EBs and RBs are two developmental forms characterized by profound differences in membrane composition and structure that play an important role in the efficiency of bacterial lysis during DNA and RNA extraction procedures. Several lysis protocols compatible with the Promega Wizard SV Genomic DNA Purification kit have been evaluated on samples collected at different times corresponding to the different developmental stages that characterize the growth of *Parachlamydia* within *A. castellanii*. These experiments showed that a specific lysis protocol including an incubation of 2 h with proteinase K at 55 °C has to be followed to ensure efficient lysis of both EBs and RBs since an incomplete lysis of EBs was obtained in the absence of proteinase K treatment as measured by quantitative real-time PCR of the 16S rRNA gene (Figs 2 and S2). Thus, a reduced amount of 16S rRNA gene was observed in the absence of proteinase K treatment for samples collected during early (0–4 h postinfection) and late phases (36–48 h postinfection) of the replicative cycle that are characterized by a significant presence of EBs, whereas no difference was measured during the mid-phase (8 h to 24 h), which is characterized by the sole presence of replicating RBs.

The extraction of integral bacterial RNA is incompatible with proteinase K treatment at 55 °C for 2 h. Thus, the

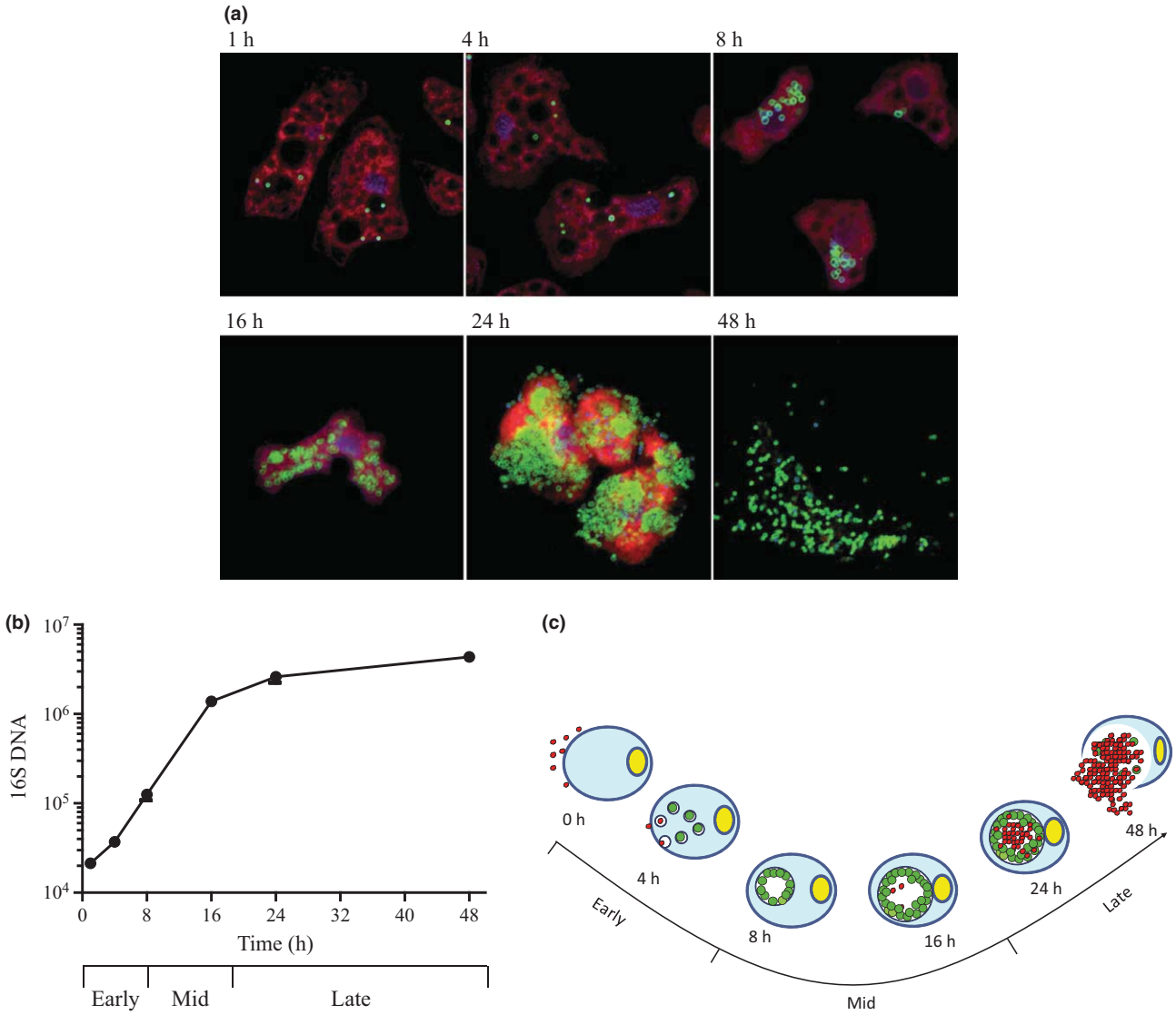

Fig. 1 Temporal characterization of the replicative cycle. (a) *Acanthamoeba castellanii* were infected with *Parachlamydia acanthamoebae* at a MOI of 10 to obtain an amebal infectious rate of nearly 100% ensuring that only a single infectious cycle occurred in every experiment. Samples were collected at the indicated times postinfection to cover the complete replicative cycle. Bacteria (green) were labeled by immunofluorescence using specific mouse anti-*P. acanthamoebae* polyclonal antibodies. *Acanthamoeba castellanii* (red) were stained with concanavalin A. An average of 2–5 infectious particles per amebal cell were observed 1 h postinfection. Internalization and differentiation of EBs into RBs occurred during the 5 first hours of the infection. Replicating RBs located in bacterial inclusions were observed from 8 to 24 h postinfection. Redifferentiation of RBs into EBs occurred between 24 and 48 h postinfection. Finally, cell lysis and extrusion of infectious EBs from host cells were observed 48 h postinfection. (b) Bacterial growth measured by qPCR of the 16S rRNA gene. A lag phase corresponding to bacterial differentiation of EBs to RBs is observed during the first 5 h of infection followed by an exponential bacterial growth. An entry into stationary phase was measured between 16 and 24 h postinfection. (c) The replicative cycle was classified in three phases: Early, mid, and late. The early cycle is characterized by the differentiation of EBs into RBs. Bacterial replication and exponential growth occur during the mid-phase. The late-phase is characterized by an entry into stationary phase during which RBs redifferentiate into EBs and by the final cell lysis and release of EBs into the extracellular milieu.

transcriptional expression measured by qRT-PCR of several putative constitutively expressed housekeeping genes including *16S rRNA*, *gyrB*, *secY*, *rpoB*, and *hsp60* was compared with the amount of 16S rRNA gene extracted without proteinase K and measured by qPCR during a replicative cycle of *Parachlamydia* in *A. castellanii* (Fig. 2). The fold increase in the different RNAs compared with the 16S rRNA gene showed that only the *16S rRNA* was constitutively expressed during a replicative cycle (Fig. 2a). The ratio *16S rRNA*/16S rRNA gene was of about 1 at each time measured during a replicative cycle, whereas the ratio observed between other transcripts with the 16S rRNA gene was greatly varying during the infectious cycle (Fig. 2b). Thus, the normalized expression of *gyrB*, *secY*,

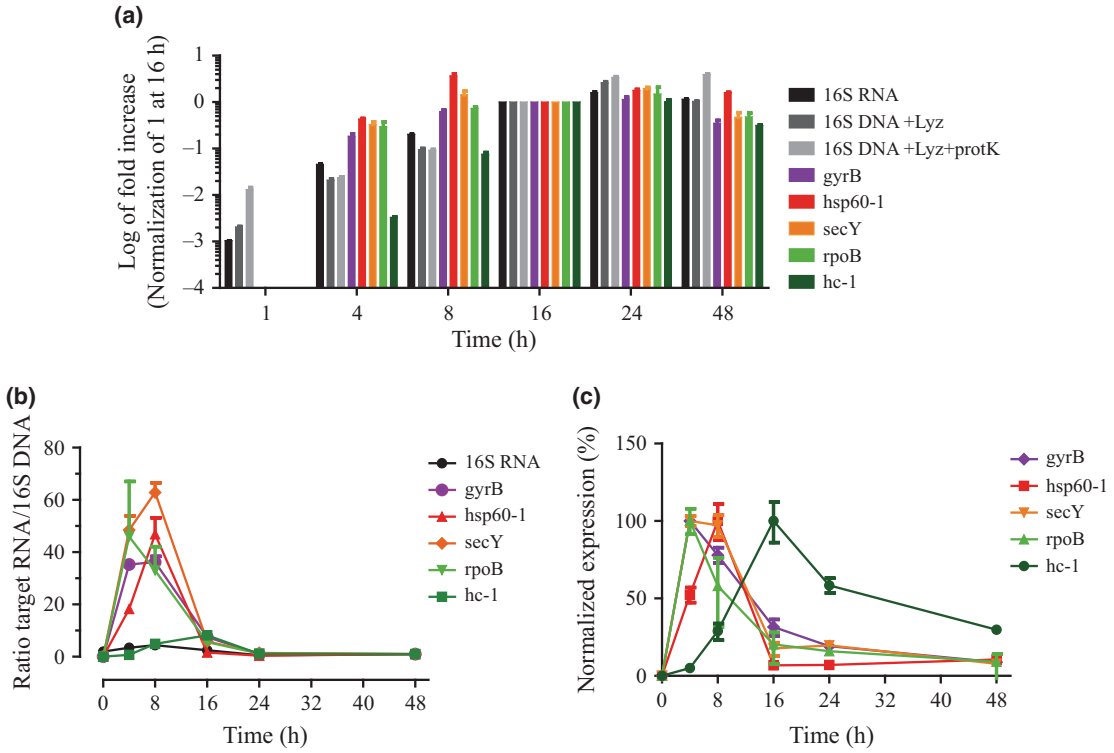

Fig. 2 Expression analysis of several housekeeping genes during an infectious cycle to identify the optimal internal control for qRT-PCR. (a) Fold increase in *16S rRNA*, *gyrB/hsp60-1/secY/rpoB/hc-1* mRNA transcripts and of 16S rRNA gene during a replicative cycle of *Parachlamydia* within *Acanthamoeba castellanii*. DNA extraction was performed with (16S DNA + Lyz + protK) and without proteinase K (16S DNA + Lyz) to obtain DNA extraction method similar to RNA extraction, which cannot be performed with proteinase K treatment. Proteinase K treatment is essential to obtain complete lysis of EBs. The fold increase was normalized to 1 at 16 h since no difference between samples treated with and without proteinase K is observed at 16 h postinfection when the bacterial population is only composed of RBs as shown in Fig. S2. (b) The ratio between *16S rRNA*, *gyrB/hsp60-1/secY/rpoB/hc-1* RNA, and 16S rRNA gene was calculated at each time and showed that only *16S rRNA* is expressed constitutively by exhibiting a ratio *16S rRNA*/16S rRNA gene of about 1 at each time of the replicative cycle. (c) Temporal transcriptional expression of *gyrB/hsp60-1/secY/rpoB/hc-1* normalized to the expression of the internal control *16S rRNA*. A significant increase in expression of the essential housekeeping genes *gyrB/hsp60-1/secY/rpoB* is observed during the early to mid-phase of the replicative cycle when EBs differentiate into RBs and during the first phase of exponential bacterial growth. As previously shown in *Chlamydia trachomatis*, the gene encoding for the histone-like protein Hc-1 exhibits an increased expression in the late mid-phase when RBs redifferentiate into EBs.

rpoB, and *hsp60* relatively to *16S rRNA* demonstrated that the expression of these essential housekeeping genes is rapidly induced following bacterial internalization (Fig. 2c). The transcriptional expression of these genes is then decreasing during the late mid-phase of the replicative cycle when bacteria begin to convert from RBs to EBs. As a control, the transcriptional expression of *hc-1*, the homolog of *Chlamydia trachomatis hctB* expressed during RB to EB conversion, was measured during a replicative cycle (Fig. 2). Similar to *hctB*, *hc-1* exhibited an increased expression in the late mid-phase corresponding to the beginning of redifferentiation of RBs into EBs. Together, these data indicate that the amount of measured *16S rRNA* transcripts reflects bacterial growth and can be thus considered as an optimal internal control to measure relative transcriptional expression of the T3SS genes of *Parachlamydia* during a replicative cycle within *A. castellanii.*

Temporal transcriptional expression of T3SS components

Similar to other *Chlamydiae*, genes encoding for T3SS apparatus components are located in distinct genomic clusters distributed along the chromosome (Fig. 3a). Four genomic clusters containing conserved genes encoding for the injectisome and the translocon apparatus and exhibiting a very similar genetic organization than other *Chlamydiae* were identified in the genome of *Parachlamydia* (Greub *et al.*, 2009). Unlike *Chlamydiaceae*, no gene showing homology with the flagellar system and having a possible function in chlamydial T3SSs has been identified in the genome of *Parachlamydia*. Thus, the transcriptional expression of the mRNA transcripts of every gene encoding a protein with a known function was analyzed by qRT-PCR (Fig. 3b). The expression of the various T3SS genes during the developmental cycle could be

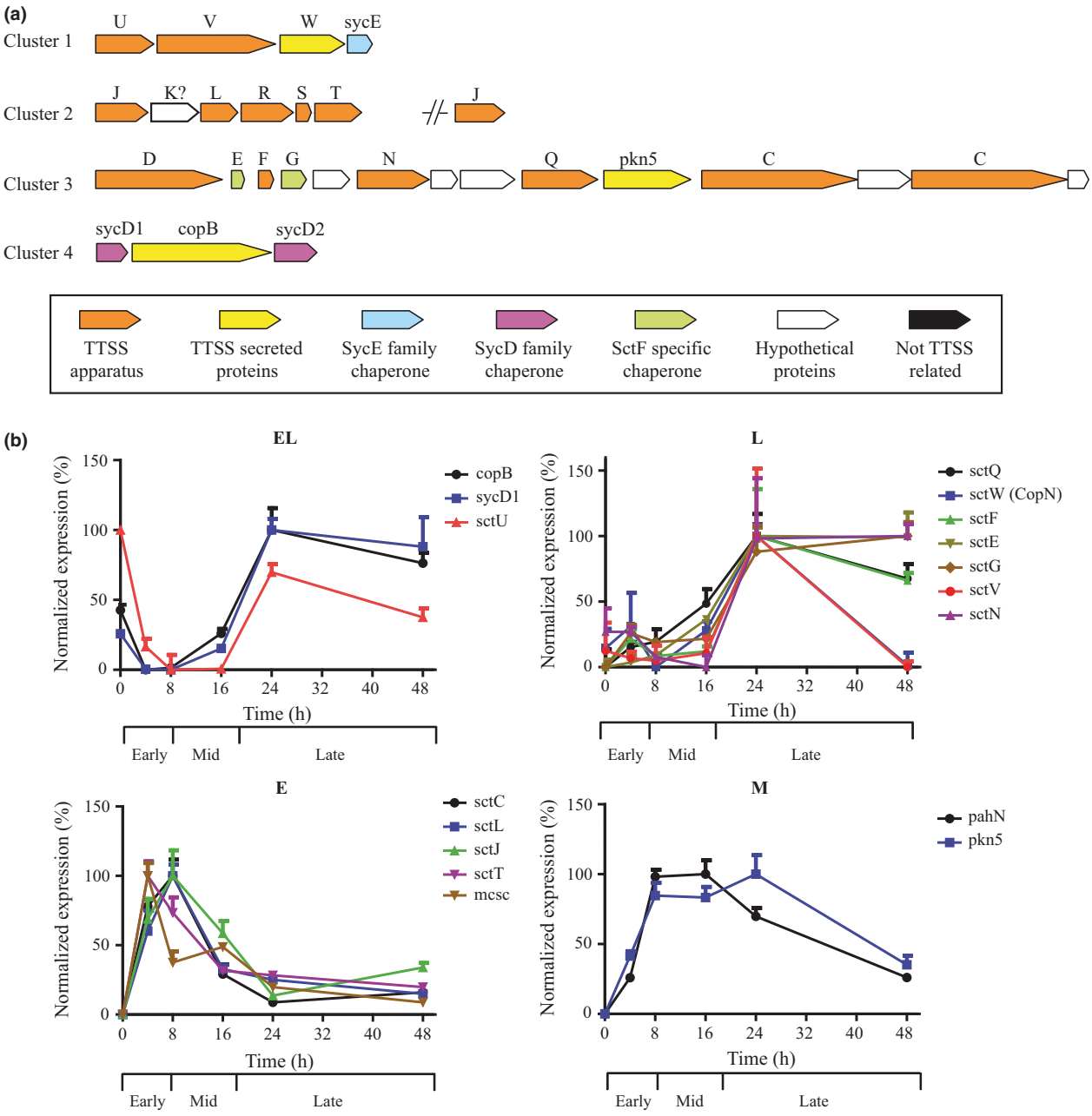

Fig. 3 Temporal transcriptional expression of T3SS genes. (a) Genetic organization of identified T3SS genes [adapted from (Greub *et al.*, 2009)]. The identified genes encoding for *Parachlamydia* T3SS proteins are localized in four main defined genomic clusters. Clusters 1–3 are much conserved among *Chlamydiales* bacteria. A difference is observed for the cluster 4 between *Chlamydiaceae* and other sequenced *Chlamydia*-related bacteria. The conserved genes are represented by different colors according to their respective functions. Hypothetical proteins are represented in light gray, and genes encoding for proteins with identified functions likely not involved in T3SS are represented in dark gray. Capital letters refer to sct gene named according to the unified nomenclature suggested by Hueck (1998). *sycE* and *sycD*: genes encoding for SycE-like and SycD/LcrH-like T3SS chaperones. All SycD-/LcrH-predicted T3SS chaperones contain conserved tetratricopeptide repeats domains. Unlike *Chlamydiaceae*, no genes showing homology with the flagellar system that could have a possible function in chlamydial T3SS have been identified. (b) Transcriptional expression of conserved T3SS genes measured by qRT-PCR. The mRNA expression of the various T3SS genes was classified in four temporal clusters: EL (early-late phase), L (late-phase), E (early phase), and M (mid-phase) according to the temporal pattern of expression during the replicative cycle. The cluster EL exhibits a marked reduction in mRNA amount during the mid-phase followed by an increased expression in late-phase. Cluster L is characterized by a basal expression during early and mid-phase and a significant increase in expression during the late-phase. Cluster E is composed of genes that are transcribed during the early and beginning of mid-phase. Finally, the cluster M includes genes that are expressed in the mid-phase.

classified in 4 temporal expression clusters (Fig. 3b). The first cluster composed of the *copB*, *sycD1*, and *sctU* is characterized by a marked repression or lack of activation during the early and mid-phases followed by a significant increased expression in the late phase (Fig. 3b, EL). The second cluster including the *sct Q/W/F/E/G/V/N* genes is characterized by a basal expression during the early and mid-phases and a significant increased expression during the late phase (Fig. 3b, L). The third cluster composed of *sctC/L/J/T* and the multicargo secretion chaperone *mcsc* includes genes that exhibit a dramatic increased expression in the early and mid-phases followed by a decreased basal expression during the late phase (Fig. 3b, E). Finally, the fourth temporal cluster is composed of the putative predicted T3SS-secreted effector *pkn5* and of a *Parachlamydia* secreted protein localizing to the replicative inclusion membrane (PahN) that are both significantly highly expressed during the mid-phase and beginning of late phase (Fig. 3b, M).

Following normalization of expression with the highest temporal expression assigned to 100 and the lowest to 0, a temporal matrix composed of the transcriptional expression of the measured T3SS genes was generated (Fig. 4a). Thus, these analyses strongly suggest that the expression of the genes that encode for T3SS components can be classified in four major defined temporal classes of gene expression composed of early (E)-, early-late (EL)-, mid (M)-, and late (L) phase-expressed genes. Early-expressed genes (E) show an induced expression during the early phase of infection characterized by bacterial internalization into host cells and differentiation of EBs into RBs. Early-late phase-expressed genes (EL) exhibit the highest amount of mRNA transcripts during both the early and late phases but display a very low level expression during the mid-phase. Mid-phase-expressed genes (M) are induced during the mid-phase of the replicative cycle corresponding to bacterial exponential growth, and late-phase-expressed genes (L) exhibit the highest level of expression during the late phase of the replication characterized by redifferentiation of EBs into RBs.

A bioinformatic analysis of the T3SS genomic clusters loci was performed with the fgenesB software to predict transcriptional units and compared with mRNA expression analysis of T3SS genes. Except for one gene (*pkn5*), the experimental qRT-PCR gene expression data are congruent with the *in silico* prediction (Fig. 4b), showing no discrepancies between temporal gene expression and association to a predicted transcriptional unit. Thus, *sctU* and *sycD1/copB* (cluster EL), *sctC* and *sctJ/L/T* (cluster E), *sctE/F/G/N/Q* (cluster L), and *sctV/sycE* (cluster L) are all located in distinct transcriptional units corresponding to defined temporal clusters (Fig. 4). Moreover, the *C. trachomatis* T3SS genes transcriptional expression study performed by Hefty *et al.* (Hefty & Stephens, 2007) strongly indicates that transcriptional expression units of T3SS genes are highly similar between *Parachlamydia* and *C. trachomatis* (Fig. 4b). Together, these data suggest that T3SSs in *Chlamydiales* are conserved not only at the level of genetic sequence and organization, but also at the level of gene expression.

Temporal protein expression measurement by Western blotting: limitations of the technique

Even though transcription and translation in bacteria are very often coupled, an analysis of protein expression

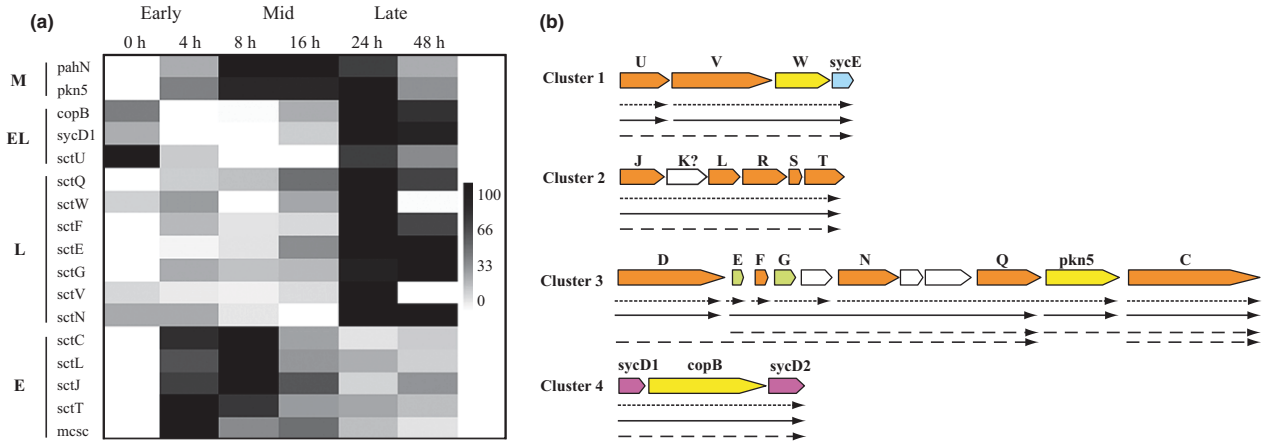

Fig. 4 Transcriptional expression cluster analysis of T3SS genes. (a) The highest degree of expression of each gene measured at different time of the infectious cycle was normalized to 100 and the lowest to 0 to generate a matrix of transcriptional expression. The four cluster of temporal expression (EL, L, E, and M) are indicated on the left part of the matrix. (b) Transcriptional units prediction. A bioinformatic analysis of the T3SS genomic clusters was conducted with the fgenesB software to predict transcriptional units (dotted arrows). Transcriptional units deduced from the experimental transcriptional expression analysis by qRT-PCR (solid arrows). Each gene associated with a predicted transcriptional unit belongs to the same temporal expression cluster. Operon prediction of *Chlamydia trachomatis* genomic loci containing T3SS genes as described by Hefty *et al.* (Hefty & Stephens, 2007) (dashed arrows). The transcriptional units predicted by the temporal transcriptional clustering of *Parachlamydia* are in congruence with the transcriptional unit prediction of the fgenesB software analysis and are highly similar to the operon prediction described in *C. trachomatis*.

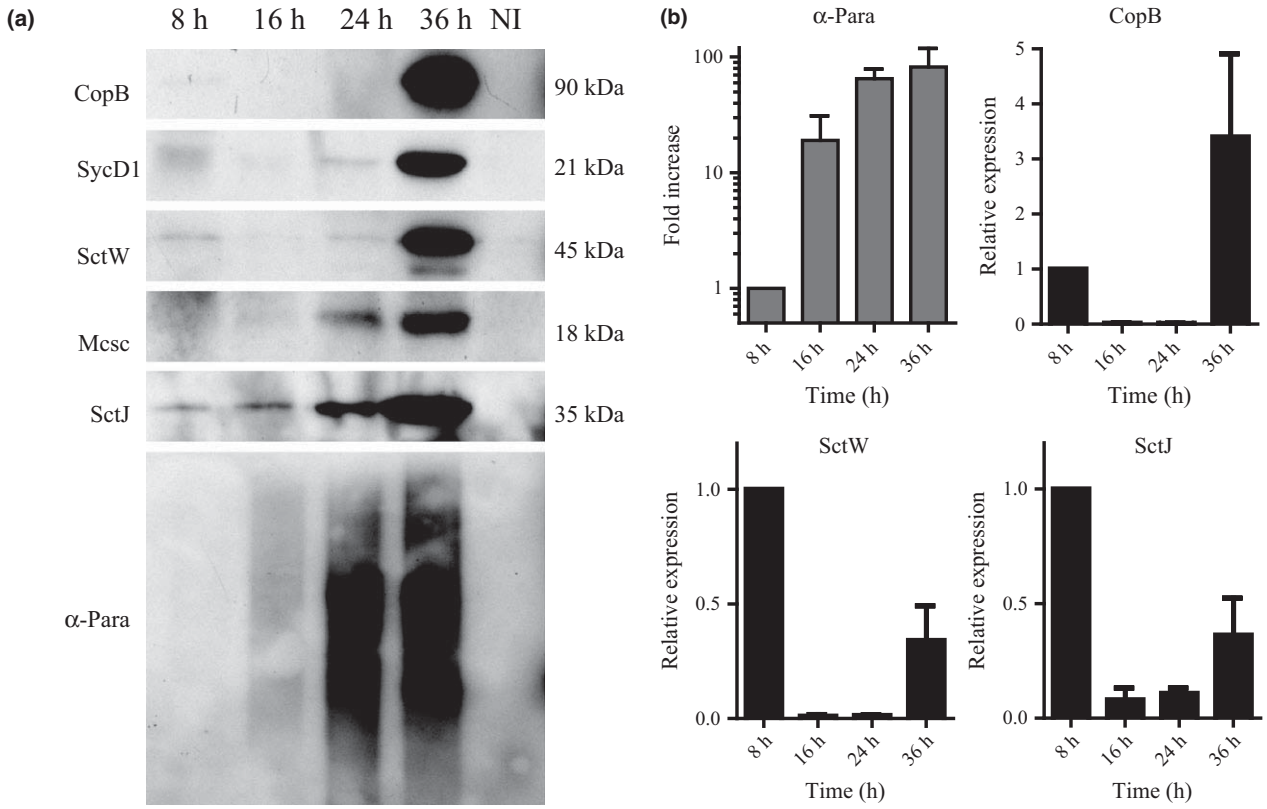

Fig. 5 Protein expression analysis by Western blot. (a) The amount of the T3SS proteins Mcsc, SctJ, SctW (CopN), CopB, and SycD was analyzed at different times postinfection by Western blot using specific mouse antisera. A polyclonal mouse antisera directed against whole bacterial cells (α-Para) was used as an internal control to estimate bacterial number at each time collected during the infectious cycle. NI: *Acanthamoeba castellanii* noninfection control. (b) The relative expression of CopB, SctW (CopN), and SctJ at different times of bacterial growth was estimated by calculating the ratio between the intensity of the bands corresponding to the different proteins and the intensity of the signal obtained with total anti-*Parachlamydia* antisera (α-Para). The results were normalized to 1 at 8 h postinfection. The expression of SycD and Mcsc was not or poorly detected at 8 h and 16 h, hindering the possibility to measure their relative protein expression during the infectious cycle by Western blot. Thus, the expression of the protein CopB is induced in the late-phase of the replicative cycle. SctW (CopN) exhibits a significant increased level 36 h postinfection corresponding to a late-phase expression, but the protein is also present in high concentrations at 8 h postinfection. A high level of SctJ is detected at 8 h postinfection corresponding to the early/mid-phase of the replicative cycle.

throughout an infectious cycle has to be performed to confirm that a similar temporal expression of T3SS genes and their respective encoded proteins is observed. Proteins encoded by genes belonging to different temporal clusters were selected for protein purifications and mouse immunization programs. Two proteins, Mcsc and SctJ, encoded by genes expressed during early and mid-phase (temporal cluster E), two proteins, CopB and SycD1 (Scc2), encoded by genes expressed during the early and late phase (temporal cluster EL), and CopN (SctW) encoded by a gene expressed during the late phase (temporal cluster L) were selected. The antisera specificity and the protein expression at different times of the infectious cycle were measured by Western blot using specific antibodies (Fig. 5a). A major drawback of measuring comparative protein amounts during the bacterial growth of obligate intracellular bacteria is the difficulty to normalize the amount of total bacterial proteins collected at different times during the replication cycle. An increase in specific proteins amounts in the late phase of the replicative cycle may only be due to a significant increase in bacterial numbers and not due to a specific up-regulation of protein expression. Thus, specific antiserum raised against whole bacterial cells was used as an internal control to monitor bacterial growth during the development cycle. The expression of SycD1 and Mcsc was poorly or not detected by Western blot before the late phase of the replicative cycle hindering the possibility to measure their relative expression throughout parachlamydial growth within *A. castellanii*. An estimation of the relative expression of CopB, CopN (SctW), and SctJ during the infectious cycle was calculated by normalizing the measured intensity of the band corresponding to the various proteins to the intensity of the signal corresponding to the whole bacterial cells (Fig. 5b). Similar to gene expression analysis of *copB* and *copN (SctW)*, an increasing amount of the protein CopB and CopN (SctW) was observed in the late phase of the bacterial replicative

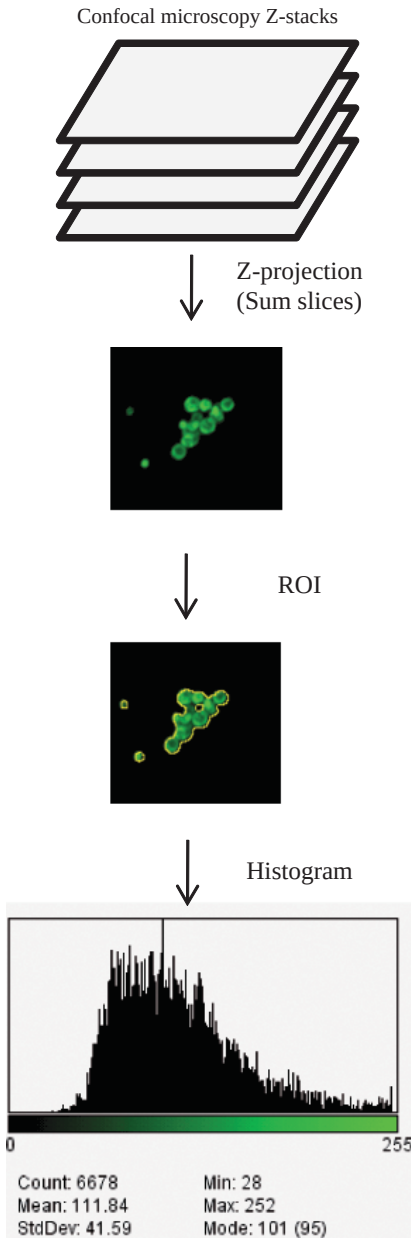

Fig. 6 Quantitative immunofluorescence microscopy. Proteins are labeled by immunofluorescence staining with specific mouse polyclonal antibodies. A series of images of multiple focal planes covering the entire thickness of the sample were collected by *z*-stack confocal microscopy. Using the ImageJ software, a *Z* projection composed of the summing of the slices is generated. The ROI including only the signal of intensity emitted by the bacteria is defined. A histogram of the ROI composed of the signal intensity on the *x*-axis and of the frequency on the *y*-axis is generated. A mean value and a standard deviation of the histogram of the frequency distribution of fluorescence intensity are also generated. This method allows the accurate measurement of protein expression at the single-cell level.

cycle. Interestingly, a high relative amount of these proteins was also observed at 8 h suggesting that late-phase-synthesized proteins of the T3SS are likely functional and still present in high amount during the early phase of subsequent infection cycles. The protein encoded by the early-transcribed gene *sctJ* exhibited the highest relative expression at 8 h confirming that *de novo* SctJ protein synthesis is likely occurring during the early phase of the infection (Fig. 5b). Unfortunately, the amount of bacteria present during the very early phase of infection is very low, and the expression of the analyzed proteins was not detected before 8 h postinfection, hindering the possibility to accurately monitor protein expression by Western blot during the critical first hours of the infectious cycle. In addition, the relative intensity measured at early time of infection by Western blot is subjected to imprecision due to very low signal detection. Thus, an alternative method to obtain more accurate protein expression measurement during the entire replicative cycle is required.

Temporal protein expression measurement by quantitative immunofluorescence

To circumvent Western blotting experimental limitations, a quantitative immunofluorescence method proposed by Noursadeghi *et al.* (Noursadeghi *et al.*, 2008) was adapted to measure bacterial single-cell protein expression by quantitative immunofluorescence confocal microscopy (Fig. 6). This method relies on the measurement of the summing of protein signals from multiple focus plans covering the entire thickness of the sample. Quantitative fluorescence data are then obtained by generating the histogram of the signal intensity of a *Z* projection obtained by summing multiple focal slices. Using this methodology, the protein expression of the late-cycle-expressed gene *copB* was analyzed during a complete replicative cycle using a specific anti-CopB mouse antisera (Fig. 7). Quantitative immunofluorescence histograms were generated for several time points postinfection and showed that the protein CopB is expressed during late-phase cycle, confirming a late-phase cycle expression of the T3SS component CopB. The same analysis was applied to the Mcsc, SctJ, PahN, and SctW (CopN) proteins (Fig. 8). Similar to CopB, the temporal expression of these four proteins was congruent with the temporal expression of their respective mRNA transcripts (Figs 8 and 3b). The chaperone Mcsc and the IM components SctJ were expressed in higher amount 2 h and 8 h postinfection, during the early and mid-phase cycles, followed by a marked reduced signal intensity observed from 16 h postinfection, which corresponds to the entry into late-phase cycle. The histogram intensity of the late-transcribed gene-encoded protein SctW (CopN) showed a gradual reduction in the protein amount from 2 h to 16 h, indicating that a relative high amount of proteins are present in EBs and in early-differentiated RBs during the first phase of the infectious cycle, but that no significant induction of protein expression occurred before 24 h postinfection, which corresponds to a late-phase protein expression. Finally, the protein PahN encoded by a mid-phase-transcribed gene showed also an increased expression from 8 h postinfection, which is maintained

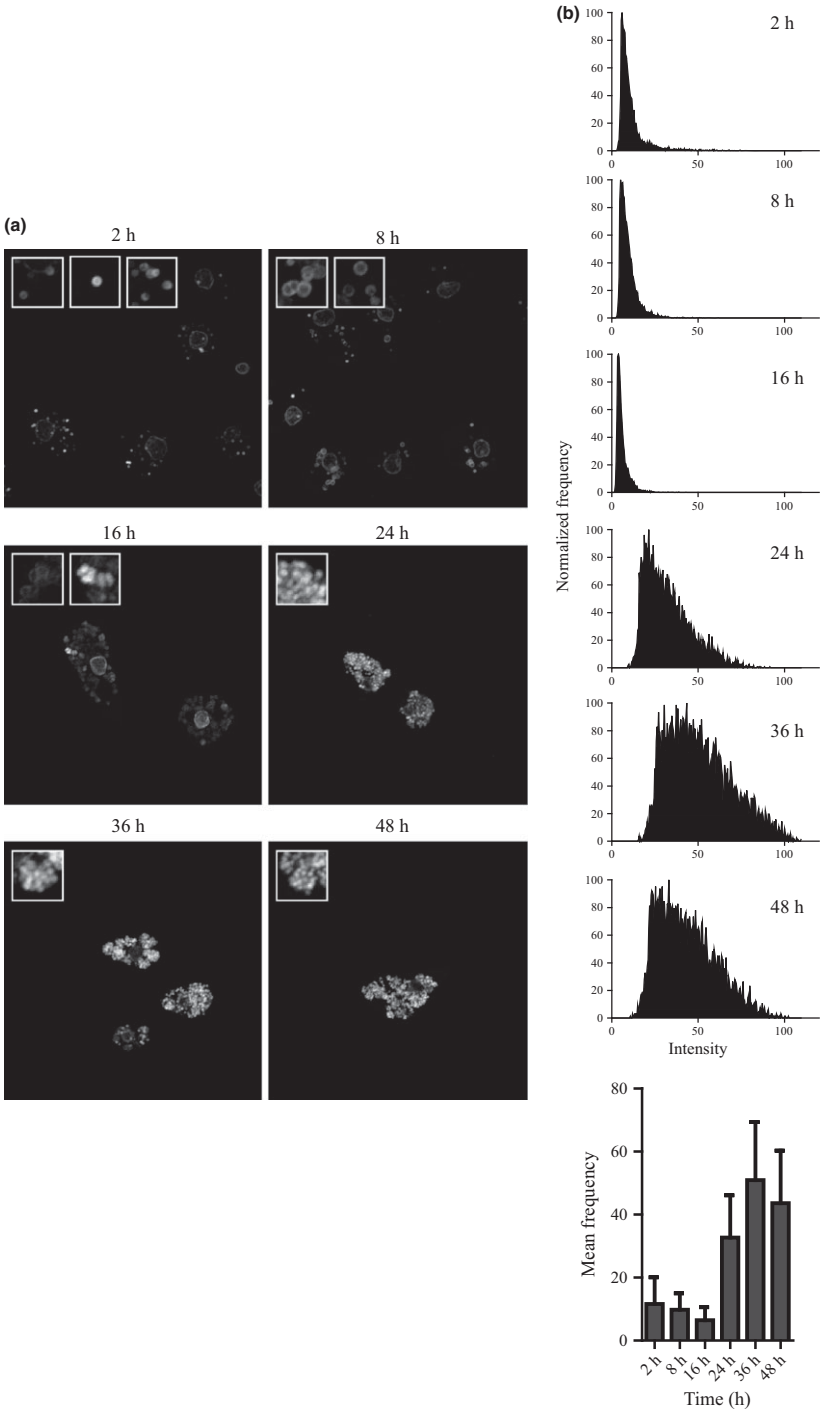

Fig. 7 Protein expression analysis of the late-phase-transcribed gene *copB*. CopB was detected with a specific mouse antisera by immunofluorescence staining. (a) *Z* projection images generated at different times during infection. Each image contains magnification of various levels of CopB expression observed in different bacteria. At 2 h postinfection, a heterogenous CopB expression is observed among EBs. Most bacteria exhibit a low CopB expression with only a minor subset showing moderate-to-high protein expression. CopB expression remains low at 8 h postinfection with some RBs expressing CopB moderately. At 16 h postinfection, the majority of bacteria poorly expressed CopB, but patches of bacteria likely located in the same inclusion exhibit significant increased level of expression. At 24 h, 36 h, and 48 h postinfection, most bacteria highly expressed CopB. (b) Histograms of the frequency distribution of fluorescence intensity were generated with each *Z* projection showed in panel A. The mean frequency for each histogram was also calculated. These data demonstrate that bacteria induced CopB expression at about 24 h postinfection, which corresponds to the transcriptional temporal expression of the *copB* gene (Fig. 3b).

during the mid- to late phase of the replicative cycle. These data demonstrate that the temporal pattern of protein expression measured by quantitative immunofluorescence of the five selected proteins Mcsc/SctJ/CopB/SctW/PahN is similar to their respective mRNA temporal expression measured by qRT-PCR. These data indicate that protein and mRNA expression of various T3SS components are tightly coupled and that temporal transcriptional expression analysis of multiple T3SS genes can be used to monitor the expression of different T3SS components and thus to characterize its functionality during an infectious cycle.

Discussion

Genome sequencing of multiple *Chlamydiales* bacteria belonging to different distant families has demonstrated that despite marked differences in their genomic size and

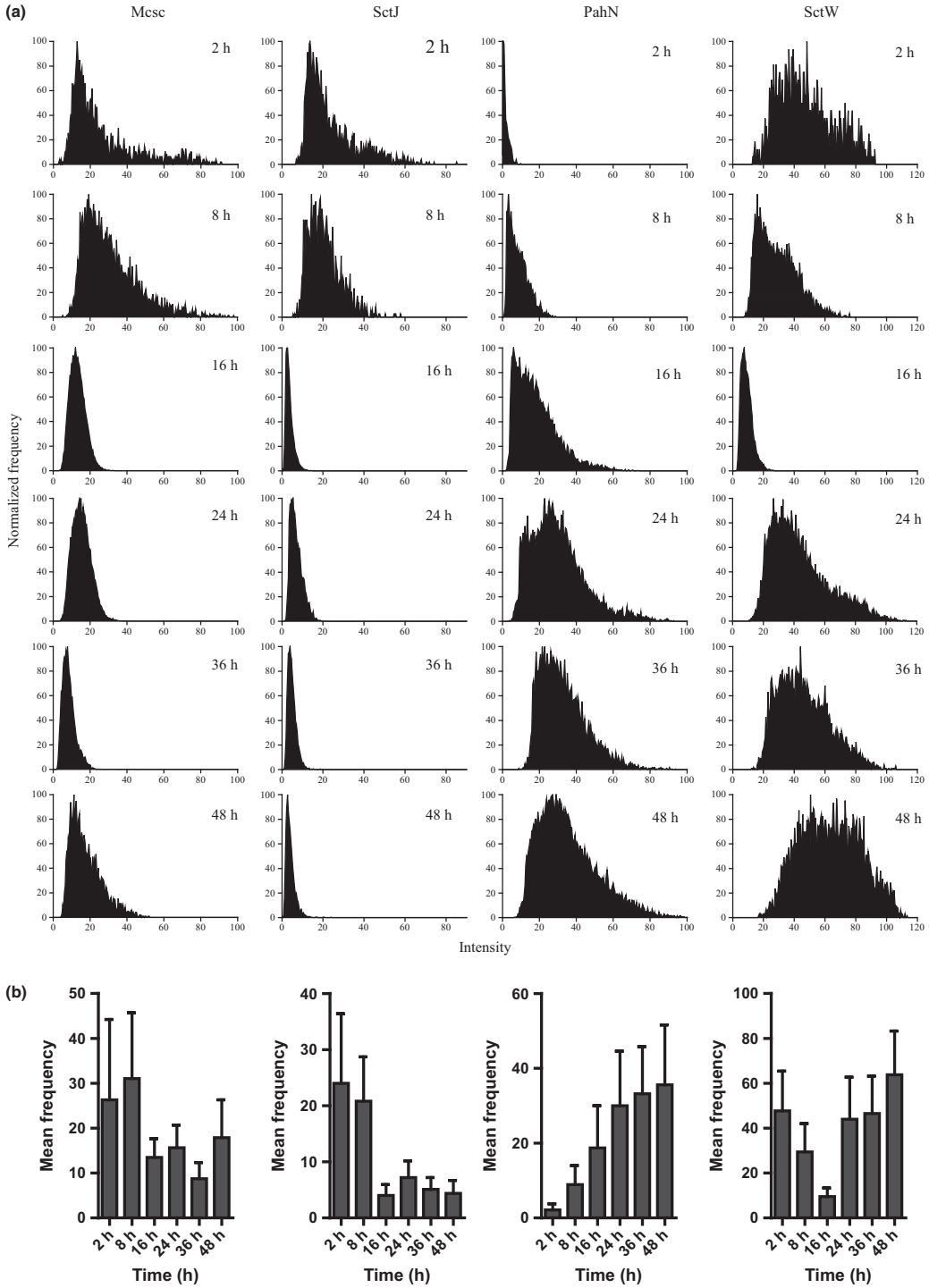

Fig. 8 Protein expression analysis of Mcsc, SctJ, PahN, and SctW (CopN). Two proteins (Mcsc and SctJ) encoded by genes that are transcribed during the early and mid-phase, one protein (PahN) encoded by a mid-phase-transcribed gene and one protein (SctW) encoded by a late-phase-transcribed gene were analyzed by quantitative immunofluorescence. Similar to transcriptional expression, the Mcsc and SctJ protein exhibit an early to mid-phase increased protein expression at 2 h and 8 h postinfection followed by a reduced expression during the mid to late-phase of the infection cycle. The expression of the PahN protein was induced during mid-phase and remained highly expressed throughout the rest of the infectious cycle. Relative high amount of SctW was measured 2 h postinfection followed by a gradual decrease in protein levels until 16 h postinfection. A significant increase in protein expression is then observed in the late-phase cycle at about 24 h postinfection, which corresponds to transcriptional expression of the *sctW* gene.

content, the T3SS loci distributed in different clusters along the chromosomes exhibit a conserved sequence and genetic organization (Peters *et al.*, 2007; Greub *et al.*, 2009; Bertelli *et al.*, 2010; Collingro *et al.*, 2011). Several studies have demonstrated that specific inhibition of T3SS with chemical compounds totally inhibits bacterial growth in a dose-dependent manner, strongly indicating that this secretion system is essential for the establishment of *Chlamydiales* replicative conditions (Muschiol *et al.*, 2006; Bailey *et al.*, 2007; Bertelli *et al.*, 2010). The temporal expression of T3SS during a replicative cycle has only been studied in *Chlamydiaceae* including *C. trachomatis*, *C. pneumoniae*, and *C. psittaci*. In this study, a complete characterization of the temporal expression of multiple T3SS components at the transcriptional and protein level has been performed in *P. acanthamoebae* replicating in its natural host cell *A. castellanii*. This study is the first description of the T3SS expression during the replicative cycle of a member of the *Chlamydiales* order not belonging to the *Chlamydiaceae* family. The replicative cycle of *Parachlamydia* within *A. castellanii* was separated in three phases, early, mid, and late. The early phase is characterized by a lag phase when EBs are internalized in the host cell and differentiate into RBs. The mid-phase is characterized by exponential bacterial replication. The late phase is starting when bacteria enter stationary phase where RBs redifferentiate into EBs that are then released in the extracellular milieu. This study showed that the temporal transcriptional expression of multiple genes encoding for T3SS components could be classified in four different temporal clusters depending on their pattern of expression during the early, mid- and late phases of an infectious cycle. Classical Western blotting being of limited value for quantitative temporal assessment of protein expression of obligate intracellular bacteria, a new quantitative immunofluorescence approach allowing accurate measurement of protein expression was used in this study. The expression analysis of selected T3SS proteins encoded by genes belonging to different temporal clusters showed that a similar temporal pattern of transcriptional and protein expression was observed for each of these genes (*copB, mcsc, sctJ, pahN, sctW*).

Based on our experimental data, a model of temporal expression of T3SS during an infectious cycle can be proposed (Fig. 9). The T3SS is a multicomponent complex machinery containing protein with diverse functions and in varying quantities. A varying stoichiometric composition of the T3SS could likely define the functionality of the apparatus. The levels of proteins in bacterial cells are controlled by multiple mechanisms and are defined by both the rate of protein synthesis and protein degradation, which are varying with the physiological status of the bacteria during a growth cycle. The relative protein content of the T3SS in EBs is likely similar to the protein content observed during the late phase of the replicative cycle when RBs redifferentiate into EBs before cell lysis and bacterial release in the extracellular milieu. During that time, the T3SS is likely not required for secretion of bacterial effectors and maintained in a dormant state ready to be activated. Upon cell contact and bacterial internalization of EBs, the T3SS is likely quickly activated to allow rapid secretion of effector proteins to modulate host cell functions. Varying *de novo* rapid synthesis of T3SS components depending of protein stability, quantity and functionality likely occurs during the critical early phase of bacterial infection to promote bacterial survival, differentiation, maturation, and initiation of replication. The subversion of host cell defense mechanisms has likely to be operated during the early phase of the infection to ensure bacterial evasion from the lytic pathway. Similarly, a rapid modulation of host cell functions ensuring a fast maturation of the replicative vacuole is a prerequest to trigger bacterial replication. Thus, the importance of a highly functional and efficient T3SS during the early phase of infection would likely confer a significant advantage for the intracellular bacteria against the defense mechanisms of the host cell. In mid-phase, once the bacteria have established conditions allowing efficient bacterial replication such as replicative vacuole maturation, subversion of host cell defenses, and establishment of systems allowing efficient scavenging of host cell nutrients, the importance and the number of T3SS per bacteria are reduced or only maintained in bacteria being in direct contact with the inclusion membrane. Finally, increased *de novo* synthesis of some T3SS components in the late-phase triggers the shutdown of the apparatus (SctW) and the formation of a silent T3SS in EBs ready to be rapidly activated when requested.

A significant similarity between the transcriptional expression units of *Parachlamydia* and *C. trachomatis* was observed, suggesting that T3SSs sequences, genetic organization, and transcriptional expression units are highly conserved among *Chlamydiales* bacteria (Hefty & Stephens, 2007). However, several studies indicate that the temporal expression of these transcriptional units may vary among *Chlamydiales* bacteria (Slepenkin *et al.*, 2003; Lugert *et al.*, 2004; Hefty & Stephens, 2007; Beeckman *et al.*, 2008). Some discrepancies may originate from several issues including chlamydial species specificities, growth kinetics differences, host cell lines, and variation of the limit of detection of the molecular techniques used in the different experimental assets. The regulation of the T3SS expression in *Chlamydiales* is poorly understood. T3SS genes and operons are preceded by predicted *E. coli* σ70-like promoter elements, but no transcriptional regulators have yet been identified (Hefty & Stephens, 2007). Similarly, the explanation of the separation of the *Chlamydiales* T3SS elements in distinct genomic clusters and transcriptional units expressed in different temporal classes remained to be determined. Transcriptional regulation of T3SS genes in other bacterial species such as *Yersinia* and *Salmonella* is mainly controlled by AraC-like transcriptional activators whose activities are regulated by several regulatory pathways responding to multiple environmental signals sensed during the infection process (Francis *et al.*, 2002). No gene encoding for an AraC-like transcriptional activators has been identified in *Chlamydiales* genomes, suggesting that C*hlamydiales* T3SSs are regulated by a different mechanism. The absolute requirement of T3SS for chlamydial survival and replication in host cells may suggest that

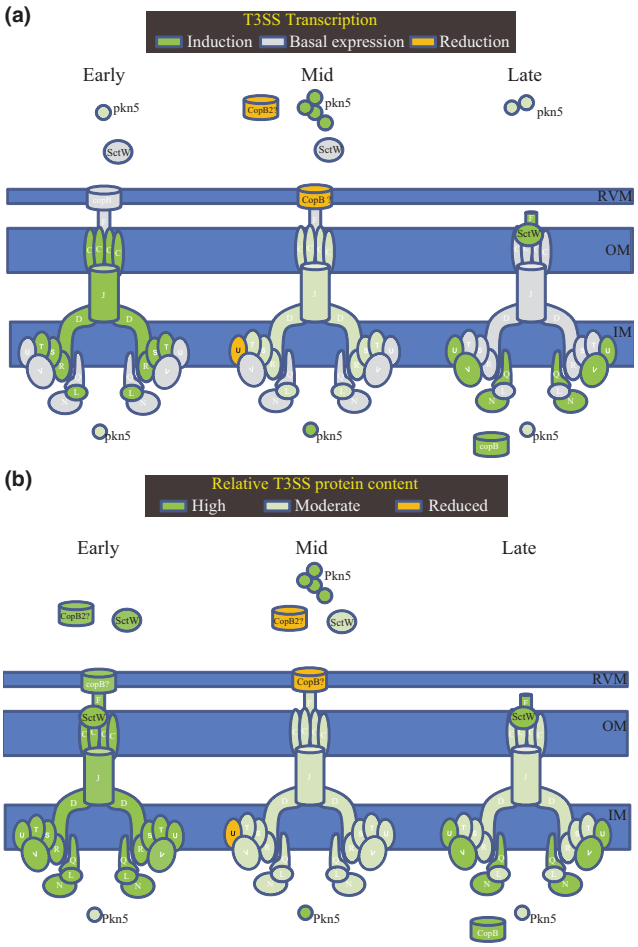

Fig. 9 Model of expression of T3SS components during an infectious cycle of *Parachlamydia* within *Acanthamoeba castellanii*. (a) Schematic overview of the transcriptional expression of the T3SS genes during the three phases of the replicative cycle. Early phase: An increased transcriptional expression of *sctC/D/J/T/S/R/L* genes is observed during the early phase of the cycle. A basal transcriptional expression is observed for the genes encoding other components of the T3SS. Mid-phase: A reduced and moderate expression of *sctC/D/J/T/S/R/L* genes is detected, while no change in basal expression of *sctV/N/Q/F/W* genes is observed. The level of *sctU/copB* transcripts is almost undetected suggesting that the transcriptional expression of these genes is highly reduced during the mid-phase of the cycle. In the contrary, the transcriptional expression of the gene encoding for the putative effector protein Pkn5 is significantly induced. Late phase: A basal expression of the genes *sctC/D/J/T/S/R/L* that were highly expressed during the early phase is observed, whereas an increased transcriptional expression of the genes *sctV/N/Q/F/W/U* and *copB* (or *CopB2*) is measured during the late phase of replication. (b) Relative T3SS proteins content during the three different phases of the cycle. The T3SS is a multicomponent complex machinery containing protein with diverse functions and in varying quantities. A varying stoichiometric composition of the T3SS could likely define the functionality of the apparatus. The levels of proteins in bacterial cells are controlled by multiple mechanisms and are defined by both the rate of protein synthesis and protein degradation, which are varying with the physiological status of the bacteria during a growth cycle. The relative protein content of the T3SS in EBs is likely similar to the protein content observed during the late phase of the replicative cycle when RBs redifferentiate into EBs before cell lysis and bacterial release in the extracellular milieu. During that time, the T3SS is likely not required for secretion of bacterial effectors and is maintained in a dormant state ready to be activated. Upon cell contact and bacterial internalization of EBs, the T3SS is likely quickly activated to allow rapid secretion of effector proteins to modulate host cell functions. Rapid *de novo* synthesis of some T3SS components likely occurs during the critical early phase of bacterial infection to promote bacterial survival, differentiation, maturation, and initiation of replication. The subversion of host cell defense mechanisms has likely to be operated during the early phase of the infection to ensure bacterial evasion from the lytic pathway. In mid-phase, once the bacteria have established conditions allowing efficient bacterial replication such as replicative vacuole maturation, subversion of host cell defenses, and establishment of systems allowing efficient scavenging of host cell nutrients, the importance and the number of T3SS per bacteria are reduced. Finally, increased *de novo* synthesis of some T3SS components in the late phase triggers the shutdown of the apparatus (SctW) and the formation of a silent T3SS in EBs ready to be rapidly activated when requested. IM: inner membrane. OM: outer membrane. RVM: replication vacuole membrane

T3SSs are controlled by the global regulatory network system of *Chlamydiales* bacteria via various transcriptional regulators and/or alternative regulatory systems. Recent data suggest that transcriptional expression of chlamydial T3SS operons is controlled by the degree of DNA supercoiling that varies temporally during a developmental cycle (Case *et al.*, 2010). Thus, the differences of sensitivity of the promoters to alteration of DNA supercoiling may define temporal transcriptional expression differences of T3SS operons and of other unrelated chlamydial genes.

The *Chlamydiales* T3SS is rapidly activated upon contact with the host cell and remains probably functional until bacterial detachment from the inclusion membrane and RBs conversion into EBs (Fields *et al.*, 2003; Clifton *et al.*, 2004; Fields & Hackstadt, 2006). Even though cell contact-dependent activation of T3SS is conserved among bacteria (Hueck, 1998), the exact mechanism governing the activation in *Chlamydiales* remains to be identified, and marked differences compared with other bacterial species T3SS could be observed considering the peculiar developmental cycle of *Chlamydiae*. For instance, the *Chlamydiales* needle protein SctF contains cysteine residues that are, like the proteins forming the envelope, linked by disulfide bridges in EBs (Betts *et al.*, 2008b), indicating that a reduction in these bonds could be required for a complete activation of the secretion. This hypothesis is supported by the observation that the classical activation of T3SSs secretion obtained by Ca^{2+} depletion did only poorly stimulated the secretion of the Tarp effector from purified cell-free *C. trachomatis* EBs (Jamison & Hackstadt, 2008).

Based on T3SS studies in other bacteria, some components of the chlamydial T3SS likely exhibit secretion regulatory functions such as SctW (CopN), SctU, and SctL. SctW contains domains similar to *Yersinia* YopN and TyeA, which are negative regulators of T3SS secretion (Goss

et al., 2004; Joseph & Plano, 2007). The secretion of effector proteins by the T3SS is partially controlled by the complex YopN/TyeA, which interacts with the secretory apparatus to prevent secretion before activation of the system upon detection of the right stimuli by the needle-tip complex (Joseph & Plano, 2007). The breaking of the YopN/TyeA interaction triggered by the stimuli that activate the T3SS induce the secretion of YopN, which render the apparatus operational for effectors secretion. The homologous SctW protein of *Chlamydiales* could have a similar regulatory function in addition of its secreted effector activity that triggers cell cycle arrest by altering the microtubule cytoskeleton (Fields & Hackstadt, 2000; Huang *et al.*, 2008). The expression of SctW observed in late-phase of the replicative cycle of *Parachlamydia* is compatible with the dual function of this protein. The expression and the recruitment of SctW to the secretory apparatus in late-phase coincide with deactivation of the T3SS and thus inhibition of secretion. During the early phase of infection, SctW is rapidly secreted, which renders again the T3SS secretion competent.

The cleavage of the SctU *Yersinia* homolog YscU is required to permit secretion of effector proteins likely by allowing the recruitment of the ATPase complex SctN/L to the apparatus (Riordan & Schneewind, 2008). The transcriptional expression of the *sctU* gene is highly reduced in the mid-phase of the replicative cycle of *Parachlamydi*a, which suggests that once the T3SS apparatus is assembled and activated, the requirement and the expression of the this protein are possibly decreased as observed in this study, or that single SctU proteins might be shared by several T3SS apparatus when its requirement decreases.

Regulation of the T3SS during the replicative cycle might be operated through the controlled temporal expression of some components required to initiate protein–protein interactions or functionality. For instance, studies on the *Yersinia* T3SS indicate that the assembly of the cytosolic complex consisting of the ATPase SctN, the interacting protein SctL, and the C ring component SctQ require the presence of all of its components (Jackson & Plano, 2000; Diepold *et al.*, 2010). Thus, in *Parachlamydia*, the late-phase cycle–expressed proteins SctN and SctQ would not be active until the early phase expression of maximal amounts of SctL initiates or increases the early formation of the SctN/SctL/SctQ complex, triggering its docking onto the IM ring and the subsequent full activation of the T3SS secretion system. Similarly, the early expression of the multiple cargo secretion chaperone Mcsc would initiate or increase a protein–protein interaction hub consisting of Mcsc–effector–SctQ complexes and activation of T3SS-dependent effector secretion.

The CopB protein identified in *Parachlamydia* is poorly homologous to the translocator proteins CopB and CopB2 of *Chlamydiaceae* bacteria (Chellas-Gery *et al.*, 2011). Similar to *sctU*, the expression of CopB is reduced during the mid-phase. Even though no sequence homologies are observed, CopB of *Parachlamydia* exhibit more similarities with the predicted secondary structures of the *C. trachomatis* CopB2 than with CopB (data not shown). In addition, no colocalization of CopB with the inclusion membrane of *Parachlamydia* has been observed in this study, suggesting that this protein is possibly secreted in the host cell cytoplasm similarly to CopB2 of *C. trachomatis* (Chellas-Gery *et al.*, 2011).

In conclusion, the differential temporal expression of T3SS components during the replicative cycle of *Parachlamydia* suggests that the maximal expression and activation of T3SS injectisomes occur during the early to mid-phase of the infectious cycle, which corresponds to a critical phase during which the intracellular bacterium has to evade and/or block lytic effectors of the amebal host cell, to differentiate from EBs to RBs, and to modulate the maturation of its replicative vacuole to create replicative condition able to sustain efficient bacterial replication. Based on several studies mainly performed in other bacteria than in *Chlamydiales*, the functions of several T3SS components are well described, whereas for other components, no functionality has yet been attributed. In addition to a described enzymatic, regulatory, or structural function, a temporal activity remains to be characterized for many proteins that compose the chlamydial T3SS machinery. The T3SS machinery is likely a dynamic structure that can fluctuate during a replicative cycle to modulate its functionality. The expression of each component of the T3SS during the replicative cycle depends on several molecular criteria including function, activity, stoichiometric ratio, stability, and turnover of each protein. In addition, some proteins might be shared between different apparatus of the cell. Finally, recent data strongly suggest that unlike other described bacterial species, the *Chlamydiales* T3SS is likely deeply involved in additional roles than solely protein secretion and translocation (Peters *et al.*, 2007). For instance, the attachment to inclusion membranes and the differentiation of RBs into EBs may be controlled by the T3SS. Thus, differential temporal expression of various components of the chlamydial T3SS may be required to modulate these multiple regulatory activities.

Acknowledgements

This work was supported by a grant from the Swiss National Science Foundation no 310030-124843 and no 310030-141050. We thank Sebastien Aeby for technical assistance. We also thank the Cellular Imaging Facility (CIF) of the University of Lausanne for confocal microscopy.

References

Bailey L, Gylfe A, Sundin C, Muschiol S, Elofsson M, Nordstrom P *et al.* (2007) Small molecule inhibitors of type III secretion in *Yersinia* block the *Chlamydia pneumoniae* infection cycle. *FEBS Lett* 581: 587–595.

Bannantine JP, Griffiths RS, Viratyosin W, Brown WJ & Rockey DD (2000) A secondary structure motif predictive of protein localization to the chlamydial inclusion membrane. *Cell Microbiol* 2: 35–47.

Beeckman DS & Vanrompay DC (2010) Bacterial secretion systems with an emphasis on the chlamydial Type III secretion system. *Curr Issues Mol Biol* 12: 17–41.

Beeckman DS, Geens T, Timmermans JP, Van Oostveldt P & Vanrompay DC (2008) Identification and characterization of a type III secretion system in *Chlamydophila psittaci*. *Vet Res* 39: 27.

Bertelli C, Collyn F, Croxatto A, Ruckert C, Polkinghorne A, Kebbi-Beghdadi C *et al.* (2010) The *Waddlia* genome: a window into chlamydial biology. *PLoS ONE* 5: e10890.

Betts HJ, Twiggs LE, Sal MS, Wyrick PB & Fields KA (2008) Bioinformatic and biochemical evidence for the identification of the type III secretion system needle protein of *Chlamydia trachomatis*. *J Bacteriol* 190: 1680–1690.

Betts-Hampikian HJ & Fields KA (2010) The chlamydial type III secretion mechanism: revealing cracks in a tough nut. *Front Microbiol* 1: 114.

Case ED, Peterson EM & Tan M (2010) Promoters for *Chlamydia* type III secretion genes show a differential response to DNA supercoiling that correlates with temporal expression pattern. *J Bacteriol* 192: 2569–2574.

Casson N, Medico N, Bille J & Greub G (2006) *Parachlamydia acanthamoebae* enters and multiplies within pneumocytes and lung fibroblasts. *Microbes Infect* 8: 1294–1300.

Casson N, Entenza JM, Borel N, Pospischil A & Greub G (2008) Murine model of pneumonia caused by *Parachlamydia acanthamoebae*. *Microb Pathog* 45: 92–97.

Chellas-Gery B, Wolf K, Tisoncik J, Hackstadt T & Fields KA (2011) Biochemical and localization analyses of putative type III secretion translocator proteins CopB and CopB2 of *Chlamydia trachomatis* reveal significant distinctions. *Infect Immun* 79: 3036–3045.

Clifton DR, Fields KA, Grieshaber SS, Dooley CA, Fischer ER, Mead DJ *et al.* (2004) A chlamydial type III translocated protein is tyrosine-phosphorylated at the site of entry and associated with recruitment of actin. *P Natl Acad Sci USA* 101: 10166–10171.

Coburn B, Sekirov I & Finlay BB (2007) Type III secretion systems and disease. *Clin Microbiol Rev* 20: 535–549.

Collingro A, Tischler P, Weinmaier T, Penz T, Heinz E, Brunham RC *et al.* (2011) Unity in variety – the pan-genome of the *Chlamydiae*. *Mol Biol Evol* 28: 3253–3270.

Cornelis GR (2002) The Yersinia Ysc-Yop 'type III' weaponry. *Nat Rev Mol Cell Biol* 3: 742–752.

Corsaro D & Greub G (2006) Pathogenic potential of novel *Chlamydiae* and diagnostic approaches to infections due to these obligate intracellular bacteria. *Clin Microbiol Rev* 19: 283–297.

Diepold A, Amstutz M, Abel S, Sorg I, Jenal U & Cornelis GR (2010) Deciphering the assembly of the *Yersinia* type III secretion injectisome. *EMBO J* 29: 1928–1940.

Fields KA & Hackstadt T (2000) Evidence for the secretion of *Chlamydia trachomatis* CopN by a type III secretion mechanism. *Mol Microbiol* 38: 1048–1060.

Fields KA & Hackstadt T (2006) The *Chlamydia* Type III secretion system: structure and implications for pathogenesis. *Chlamydia*: Genomics and Pathogenesis. (Wyrick PB & Bavoil PM, eds), pp. 219–233. Horizon Bioscience, Norfolk, UK.

Fields KA, Mead DJ, Dooley CA & Hackstadt T (2003) *Chlamydia trachomatis* type III secretion: evidence for a functional apparatus during early-cycle development. *Mol Microbiol* 48: 671–683.

Francis MS, Wolf-Watz H & Forsberg A (2002) Regulation of type III secretion systems. *Curr Opin Microbiol* 5: 166–172.

Goss JW, Sorg JA, Ramamurthi KS, Ton-That H & Schneewind O (2004) The secretion signal of YopN, a regulatory protein of the *Yersinia enterocolitica* type III secretion pathway. *J Bacteriol* 186: 6320–6324.

Goy G, Croxatto A & Greub G (2008) *Waddlia chondrophila* enters and multiplies within human macrophages. *Microbes Infect* 10: 556–562.

Greub G (2009) *Parachlamydia acanthamoebae*, an emerging agent of pneumonia. *Clin Microbiol Infect* 15: 18–28.

Greub G & Raoult D (2002) Crescent bodies of *Parachlamydia acanthamoeba* and its life cycle within *Acanthamoeba polyphaga*: an electron micrograph study. *Appl Environ Microbiol* 68: 3076–3084.

Greub G & Raoult D (2003) History of the ADP/ATP-translocase-encoding gene, a parasitism gene transferred from a *Chlamydiales* ancestor to plants 1 billion years ago. *Appl Environ Microbiol* 69: 5530–5535.

Greub G & Raoult D (2004) Microorganisms resistant to free-living amoebae. *Clin Microbiol Rev* 17: 413–433.

Greub G, Mege JL & Raoult D (2003a) *Parachlamydia acanthamoebae* enters and multiplies within human macrophages and induces their apoptosis. *Infect Immun* 71: 5979–5985.

Greub G, Berger P, Papazian L & Raoult D (2003b) *Parachlamydiaceae* as rare agents of pneumonia. *Emerg Infect Dis* 9: 755–756.

Greub G, Boyadjiev I, La Scola B, Raoult D & Martin C (2003c) Serological hint suggesting that *Parachlamydiaceae* are agents of pneumonia in polytraumatized intensive care patients. *Ann N Y Acad Sci* 990: 311–319.

Greub G, Desnues B, Raoult D & Mege JL (2005a) Lack of microbicidal response in human macrophages infected with *Parachlamydia acanthamoebae*. *Microbes Infect* 7: 714–719.

Greub G, Mege JL, Gorvel JP, Raoult D & Meresse S (2005b) Intracellular trafficking of *Parachlamydia acanthamoebae*. *Cell Microbiol* 7: 581–589.

Greub G, Kebbi-Beghdadi C, Bertelli C, Collyn F, Riederer BM, Yersin C *et al.* (2009) High throughput sequencing and proteomics to identify immunogenic proteins of a new pathogen: the dirty genome approach. *PLoS ONE* 4: e8423.

Hefty PS & Stephens RS (2007) Chlamydial type III secretion system is encoded on ten operons preceded by sigma 70-like promoter elements. *J Bacteriol* 189: 198–206.

Horn M, Collingro A, Schmitz-Esser S, Beier CL, Purkhold U, Fartmann B *et al.* (2004) Illuminating the evolutionary history of chlamydiae. *Science* 304: 728–730.

Huang J, Lesser CF & Lory S (2008) The essential role of the CopN protein in *Chlamydia pneumoniae* intracellular growth. *Nature* 456: 112–115.

Hueck CJ (1998) Type III protein secretion systems in bacterial pathogens of animals and plants. *Microbiol Mol Biol Rev* 62: 379–433.

Jackson MW & Plano GV (2000) Interactions between type III secretion apparatus components from *Yersinia pestis* detected using the yeast two-hybrid system. *FEMS Microbiol Lett* 186: 85–90.

Jamison WP & Hackstadt T (2008) Induction of type III secretion by cell-free *Chlamydia trachomatis* elementary bodies. *Microb Pathog* 45: 435–440.

Joseph SS & Plano GV (2007) Identification of TyeA residues required to interact with YopN and to regulate Yop secretion. *Adv Exp Med Biol* 603: 235–245.

Lamoth F & Greub G (2009) Amoebal pathogens as emerging causal agents of pneumonia. *FEMS Microbiol Rev* 34: 260–280.

Lugert R, Kuhns M, Polch T & Gross U (2004) Expression and localization of type III secretion-related proteins of *Chlamydia pneumoniae*. *Med Microbiol Immunol* 193: 163–171.

Mota LJ & Cornelis GR (2005) The bacterial injection kit: type III secretion systems. *Ann Med* 37: 234–249.

Muschiol S, Bailey L, Gylfe A, Sundin C, Hultenby K, Bergstrom S *et al.* (2006) A small-molecule inhibitor of type III secretion inhibits different stages of the infectious cycle of *Chlamydia trachomatis*. *P Natl Acad Sci USA* 103: 14566–14571.

Noursadeghi M, Tsang J, Haustein T, Miller RF, Chain BM & Katz DR (2008) Quantitative imaging assay for NF-kappaB nuclear translocation in primary human macrophages. *J Immunol Methods* 329: 194–200.

Peters J, Wilson DP, Myers G, Timms P & Bavoil PM (2007) Type III secretion a la *Chlamydia*. *Trends Microbiol* 15: 241–251.

Riordan KE & Schneewind O (2008) YscU cleavage and the assembly of *Yersinia* type III secretion machine complexes. *Mol Microbiol* 68: 1485–1501.

Slepenkin A, Motin V, de la Maza LM & Peterson EM (2003) Temporal expression of type III secretion genes of *Chlamydia pneumoniae*. *Infect Immun* 71: 2555–2562.

Subtil A, Delevoye C, Balana ME, Tastevin L, Perrinet S & Dautry-Varsat A (2005) A directed screen for chlamydial proteins secreted by a type III mechanism identifies a translocated protein and numerous other new candidates. *Mol Microbiol* 56: 1636–1647.

Supporting Information

Additional Supporting Information may be found in the online version of this article:

Fig. S1. The time course of the infection of *Parachlamydia* into *A. castellanii* is similar between a MOI of 1 and 10 (A) Bacterial growth measured by qPCR of the 16S rRNA gene. The MOI does not affect the time course of infection. A higher fold increase is observed with a MOI of 1 due to reinfection of uninfected amoebae occurring around 24 h postinfection. (B) Number of bacteria per amoebae at different time of infection. The number of bacteria was counted accurately until 30 bacteria per amoebae. A semi-quantitative estimation of the number of bacteria per amoebae was performed for higher number of bacteria as described in Goy *et al*. (Goy *et al*., 2008). (C) Percent of infected amoebae at different time of infection. About 97% to 100% of amoebae are infected with an MOI of 10 whereas 50% of amoebae are infected with a MOI of 1 during the first 24 hours of infection.

Fig. S2. Proteinase K treatment is required for complete EBs lysis during DNA extraction.

Table S1. List of primers used in qRT-PCR.

Table S2. Cloning primers and plasmids.